HARP Collaboration

HARP Memo 03-001
6 June 2003
revised 10 June 2003
http://cern.ch/dydak/TPCdistortions.ps

On distortions of TPC coordinates: inhomogeneities of electric and magnetic field

F. Dydak

CERN-HARP-CDP-2003-001
06/06/2003

Abstract

After a general discussion of electron drift in a gas volume with electric and magnetic fields, distortions in the r and $r \cdot \phi$ coordinates arising from inhomogeneities of the electric and magnetic fields in the HARP TPC are calculated.

Inhomogeneities of the electric field arise from

- positive ions released by cosmic rays,
- positive ions released by interaction secondaries,
- positive ions released by beam muons,
- positive ions released from beam particles downstream of the inner field cage, and
- a high voltage misalignment between the outer and inner field cages.

Also, distortions arising from the inhomogeneity of the magnetic field are calculated.

These effects resolve the controversy on unphysical numbers of 'wrong-charge' TPC tracks.

The bad news are that effects are too big to be neglected. The good news are that, with enough sweat and tears, they can be adequately corrected.

1 Introduction

The exploitation of the HARP TPC depends, *inter alia*, on a good understanding of the movement of electrons in a gas volume, over long distances, under the influence of electric and magnetic fields. While great care was taken to ensure homogeneous fields by construction, some imperfections were unavoidable (or, *nostra culpa,* crept in by mistake).

This note assesses quantitatively the effect of known inhomogeneities of the electric and magnetic fields in the HARP TPC.

In a TPC, one distiguishes between two different $E \times B$ effects:

- the 'wire' $E \times B$ effect, caused by the Lorentz-force on the electrons primarily in the space around the cathode wires and the gate wires [1]; this effect leads to an increase of the $r \cdot \phi$ resolution but does not cause a distortion of the sagitta; in this note, the 'wire' $E \times B$ effect is not considered further;
- the 'drift' $E \times B$ effect, caused by inhomogeneities of the electric and magnetic fields in the active volume of the TPV; this note is concerned with this latter effect.

The 'drift' $E \times B$ effect is in principle a serious concern in the HARP TPC, however the bulk of the problem is, by design, removed by the gating grid which prevents most of the positive ions which are generated in the amplification region, from drifting into the active TPC volume.

Below, we calculate the effects from positive ions which are created by the omnipresent cosmic rays in out-of-spill data taking; which are created during the spill by interaction secondaries; and which are created during the spill by beam muons. For all three effects, the aggravation from ion leakage arising from a finite gating grid transparency is discussed.

We also calculate the effect of positive ions which are created by non-interacting beam particles downstream of the inner field cage.

Further, we calculate the effect of an unfortunate high voltage misalignment between the outer and inner field cages.

Finally, we assess the effect of inhomogeneities of the solenoidal magnetic field.

For a discussion of the movement of electrons in gases under the influence of electric and magnetic fields, we recommend, *cum grano salis* – see below – reference [2].

2 Parameters, Constants, Conventions

In Table 1, we list parameters and constants used in this Memo (not all values are necessarily the best, but they should all be 'typical').

We use the standard HARP coordinate system: looking downstream in the $+z$ direction, the $+x$ coordinate points to the left side, and the $+y$ coordinate points upward.

Table 1: Constants and parameters

Inner radius of active TPC volume	$r_{\rm i} = 0.053$ m
Outer radius of active TPC volume	$r_{\rm o} = 0.408$ m
Length of inner fieldcage	$l_{\rm i} = 0.80$ m
Length of outer fieldcage	$l_{\rm o} = 1.54$ m
Electric field strength	$\vert\vec{E}\vert = 11000$ V/m
Magnetic field strength	$\vert\vec{B}\vert = 0.7$ T
Minimum ionizing energy loss in Ar	$\mathrm{d}E/\mathrm{d}x = 2.7 \times 10^5$ eV/m
Positive ion velocity in Ar	$v_+ = 1.7$ m/s
Electron velocity in Ar	$v_- = 5.0 \times 10^4$ m/s
Dielectric constant of the vacuum	$\epsilon_0 = 8.85 \times 10^{-12}$ F/m
$\omega\tau$	3.28 ± 0.07
Ionization potential in argon	$\sim$26 eV
Sense wire amplification	2×10^4
Spill length	0.4 s
Opening time of TPC gate	5.0×10^{-5} s
Transparency of open gate (upper limit)	0.05
Transparency of closed gate (upper limit)	0.001

The electric field vector points always to the $+z$ direction; the magnetic field vector points to the $+z$ direction when the solenoid current is set to -889.4 A in data taking with positive beam polarity [3].

The electric field never changes sign, while the magnetic field does, depending on the beam polarity.

When we look at the TPC, we always look downstream.

3 Electron drift in the active TPC volume

Since the equations in this Section are beset with many non-trivial signs of different origin, we state in detail how our equations are obtained, with a view to inviting independent cross-check.

Our *ansatz* is: let a particle with mass m and charge q move with the velocity vector $\vec{v}$ in an electric field $\vec{E}$ and a magnetic field $\vec{B}$. In the equilibrium state, the vector sum of the electric force, of the Lorentz force, and of the 'friction' force which is the average decelerating force exerted on the particle by collisions with gas molecules, will vanish. The particle's equation of motion is then

$$q \cdot \vec{E} + q \cdot (\vec{v} \times \vec{B}) - k \cdot \vec{v} = 0 \,,$$

with the phenomenological proportionality constant $k > 0$. The ratio $m/k = \tau$ has the dimension of time and characterizes the average time between successive collisions of the particle with gas molecules.

This equation can be solved for the velocity vector $\vec{v}$. The result is the 'Langevin Equation', written here intentionally in an unconventional way:

$$\vec{v} = \frac{q\tau}{m} \frac{1}{1 + (\frac{q\tau}{m})^2 |B|^2} \left(\vec{E} + \frac{q\tau}{m} (\vec{E} \times \vec{B}) + \frac{(q\tau)^2}{m^2} \vec{B} (\vec{E} \cdot \vec{B}) \right) . \tag{1}$$

In this way of writing, the dependence of $\vec{v}$ on the charge sign of the particle and on the sign of the fields $\vec{E}$ and $\vec{B}$ is transparent. We note that it is different from, for example, the signs in the pertinent article in the Particle Data Group's Review [4]. Reference [2] (where one of the authors is also co-author of the Particle Data Group article) has the same sign problem.

It is convenient to introduce two constants, the particle's cyclotron frequency (defined as positive number):

$$\omega = |(q/m)\vec{B}| ,$$

and the particle's 'mobility' (= velocity per unit electric field strength) in the absence of a magnetic field (also defined as positive number):

$$\mu = (|\vec{v}|/|\vec{E}|)_{|\vec{B}|=0} = |(q/m)\tau| .$$

Equation 1 reads specifically for an *electron*, using the constant ω throughout, as:

$$\vec{v} = -\frac{\omega\tau}{|\vec{B}|} \frac{1}{1 + (\omega\tau)^2} \left(\vec{E} - \frac{\omega\tau}{|\vec{B}|} (\vec{E} \times \vec{B}) + \frac{(\omega\tau)^2}{|\vec{B}|^2} \vec{B} (\vec{E} \cdot \vec{B}) \right) , \tag{2}$$

or with the partial use of the constant μ as:

$$\vec{v} = -\frac{\mu}{1 + (\omega\tau)^2} \left(\vec{E} - \frac{\omega\tau}{|\vec{B}|} (\vec{E} \times \vec{B}) + \frac{(\omega\tau)^2}{|\vec{B}|^2} \vec{B} (\vec{E} \cdot \vec{B}) \right) . \tag{3}$$

We assume a perfectly aligned magnetic field $\vec{B} = (0, 0, B_z)$ with $B_z > 0$, and a (nearly) parallel electric field $\vec{E} = (E_x, E_y, E_z)$ with $E_z > 0$ and with small transverse components $E_x, E_y \ll E_z$. The latter arise from ion charge build-up and/or a high voltage misalignment between the outer and inner field cages.

From Equation 3, we obtain for the components of the electron velocity vector:

$$\begin{aligned} v_x &= \frac{-\mu}{1 + (\omega\tau)^2} (E_x \mp \omega\tau E_y) \\ v_y &= \frac{-\mu}{1 + (\omega\tau)^2} (E_y \pm \omega\tau E_x) \\ v_z &= -\mu E_z . \end{aligned} \tag{4}$$

In these formulae, and in all subsequent formulae and numerical results, whenever there is a double sign the upper sign refers to the magnetic field orientation $\vec{B} = (0, 0, B_z)$ with $B_z > 0$, and the lower sign to the opposite magnet polarity.

With the angles $\alpha_x^e = E_x/E_z$, $\alpha_y^e = E_y/E_z$ and the drift length L ($L > 0$), the distortions in the pad plane are approximately (we neglect a small deviation from a straight line):

$$\begin{aligned} \Delta_x &\simeq -L \frac{1}{1+(\omega\tau)^2} (\alpha_x^e \mp \omega\tau\alpha_y^e) \\ \Delta_y &\simeq -L \frac{1}{1+(\omega\tau)^2} (\alpha_y^e \pm \omega\tau\alpha_x^e) \, . \end{aligned} \tag{5}$$

The overall negative sign appears because the drift is upstream, i.e. in the direction $-z$.

We now investigate the distortions in the pad plane arising from an inhomogeneity of the solenoidal magnetic field. For this, we assume a perfectly aligned electric field $\vec{E} = (0, 0, E_z)$ and a (nearly) parallel magnetic field $\vec{B} = (B_x, B_y, B_z)$ with small transverse components $B_x, B_y \ll B_z$ arising from unavoidable imperfections in magnet construction.

Using again Equation 3, we obtain for the components of the electron velocity vector:

$$\begin{aligned} v_x &\simeq \frac{-\mu}{1+(\omega\tau)^2} (\pm\omega\tau \frac{B_y E_z}{|B_z|} + (\omega\tau)^2 \frac{B_x E_z}{B_z}) \\ v_y &\simeq \frac{-\mu}{1+(\omega\tau)^2} (\mp\omega\tau \frac{B_x E_z}{|B_z|} + (\omega\tau)^2 \frac{B_y E_z}{B_z}) \\ v_z &\simeq -\mu \, E_z \, . \end{aligned} \tag{6}$$

With the angles $\alpha_x^m = B_x/B_z$, $\alpha_y^m = B_y/B_z$ and the drift length L, the distortions in the pad plane are approximately (again, we neglect a small deviation from a straight line):

$$\begin{aligned} \Delta_x &\simeq -L \frac{1}{1+(\omega\tau)^2} (\pm\omega\tau\alpha_y^m + (\omega\tau)^2 \alpha_x^m) \\ \Delta_y &\simeq -L \frac{1}{1+(\omega\tau)^2} (\mp\omega\tau\alpha_x^m + (\omega\tau)^2 \alpha_y^m) \, . \end{aligned} \tag{7}$$

We note that the distortions due to small transverse magnetic field components depend in a different way on $\omega\tau$ than those arising from small transverse electric field components.

4 Electric field strength from ion build-up

First we recall that the only relevant charge in the active TPC volume is due to positive ions since electrons move 3400 times faster than positive argon ions (see Table 1). The latter move slowly essentially along the electric field lines, because of their high mass, toward the high voltage membrane.

We consider four cases for the radial distribution of positive charges, $\rho(r)$:

- (a): $\rho_0^{\rm a}$, a constant volume charge density; this applies to cosmic rays;
- (b): $\rho_0^{\rm b}/r$, a volume charge density falling like $1/r$; this is used as approximation for secondary tracks from the target);
- (c): $\rho_0^{\rm c}/r^2$, a volume charge density falling like $1/r^2$; this is used as approximation for beam muons;
- (d): a linear charge density σ_0 in the central axis of the TPC; this is used for beam particles downstream of the inner field cage.

$\rho_0^{\rm a}, \rho_0^{\rm b}, \rho_0^{\rm c}$ and σ_0, respectively, are constants; r is the radius from the beam line.

The Maxwell equation for the resulting electric field is:

$$\mathrm{div}\vec{E} = \frac{\rho(r)}{\epsilon_0} \, ,$$

where $\rho(r)$ is the charge density.

This reads in cylindrical coordinates as

$$\frac{1}{r}\frac{\mathrm{d}}{\mathrm{d}r}(rE(r)) = \frac{\rho(r)}{\epsilon_0} \, .$$

When solving this differential equation, we take as boundary condition

$$\int_{r_{\rm i}}^{r_{\rm o}} E(r)\mathrm{d}r = 0 \, ,$$

where $r_{\rm i}$ is the radius of the inner field cage and $r_{\rm o}$ is the one of the outer field cage. Note that at the same depth along the TPC axis, the inner and outer field cages (should) have the same electric potential.

The solutions for the three cases (a) to (c) are:

$$\begin{aligned}
{\rm a}: \quad E(r) &= \frac{\rho_0^{\rm a}}{2\epsilon_0}\,(r - \frac{1}{2r}\frac{r_{\rm o}^2 - r_{\rm i}^2}{\ln(r_{\rm o}/r_{\rm i})}) \, ; \\
{\rm b}: \quad E(r) &= \frac{\rho_0^{\rm b}}{\epsilon_0}\,(1 - \frac{1}{r}\frac{r_{\rm o} - r_{\rm i}}{\ln(r_{\rm o}/r_{\rm i})}) \, ; \\
{\rm c}: \quad E(r) &= \frac{1}{r}\frac{\rho_0^{\rm c}}{\epsilon_0}\,(\ln r - \frac{1}{2}\frac{(\ln r_{\rm o})^2 - (\ln r_{\rm i})^2}{\ln(r_{\rm o}/r_{\rm i})}) \, .
\end{aligned} \tag{8}$$

The solution for case (d) follows from the Gauss theorem in cylindrical coordinates:

$$\mathrm{d}: \quad E(r) = \frac{\sigma}{2\pi\epsilon_0}\frac{1}{r} \, . \tag{9}$$

5 Positive ion charge densities

Table 2 gives the volume charge densities for cosmics, interaction secondaries and beam muons, and the linear charge density from beam particles downstream of the inner field cage.

For this calculation the following additional assumptions have been made beyond using numbers given in Table 1:

- Cosmics: 147 downward-going cosmic muons per m^2 and s in the upper hemisphere; 130 triggers per s;
- Interaction secondaries: 3000 interactions per spill, 5 charged secondaries per interaction (including converted γ's from π^0 decay); typical inclination 45°;
- Beam muons: 20% $\simeq$ fraction of muons in incoming beam (worst case, for low beam momenta); 0.5 $\simeq$ fraction of muons in 10 cm thick cylinder around the inner field cage;
- Downstream beam particles: 10000 beam particles per spill.

Table 2: Charge densities (all numbers in units of 10^{-10}); volume densities at the inner radius of the active TPC volume; linear charge density at the central TPC axis.

Volume charge density (C/m^3)	perfect gate	transp. open gate	transp. closed gate
Cosmics	0.0017	0.022	0.067
Interaction secondaries	1.4	42	27
Beam muons	0.087	2.7	1.7
Linear charge density (C/m)			
Beam particles	0.091		

Conclusion 1: Among the first three effects, the ion build-up from interaction secondaries is by far the largest. Cosmics can be safely neglected. Beam muons play no large rôle.

Conclusion 2: Distortions from ion build-up will primarily depend on the beam intensity, on the used target (through the conversion of γ's from π^0 decay and re-interaction of secondaries within a thick target), and on the beam momentum (through the multiplicity of secondaries).

Conclusion 3: During 2002 data taking we were (in general) careful to limit the beam intensity, during 2001 we were not; therefore, 2001 data are expected to be (much) more affected by distortions from interaction secondaries; estimates given in this note refer to typical 2002 data taking conditions.

Conclusion 4: The largest contribution arises from the transparency of the TPC gate for positive ions. When open, the gate's transparency should be smaller than 0.05 (since during the 50 μs opening time of the gate the ions drift

much less than 1 mm). When closed, the gate's transparency should be smaller than 0.001. The gate transparencies need to be known with better accuracy.

For the calculation of the resulting electric field distortions (see next section), the largest charge densities from Table 2 have been retained.

6 Transverse electric field components

Using Equations 8 and 9, the transverse electric field strengths given in Table 3 have been calculated. A positive sign of the transverse field strength means that the electric field vector points to the outer field cage; a negative sign means that it points toward the TPC axis.

There is an unfortunate high voltage misalignment between the inner and outer field cages (this was realized during the work on this Memo, on 26 May 2003). Before the start of real data taking, a comparison was made between the voltage on strip 69 of the outer field cage, and the end of the inner field cage, which should be the same. It was found that the high voltage on strip 69 was lower (in absolute value) by 1.6%. Consequently, the high voltage of the inner field cage was lowered (in absolute value) by 1.6%, with the good intention to eliminate the difference. However, the shunt resistance of 1 GΩ of the high voltage probe was overlooked – which was indeed the cause of the unexpected 1.6% drop.

Therefore, during all of HARP data taking after 8 August 2001, the high voltage of the inner field cage is lower by 1.6% than the corresponding high voltage of the outer field cage. This causes an unwanted transverse electric field component which points to the outer field cage. This component is maximal at the end of the inner field cage, and decreases linearly to zero toward the pad plane. It is absent downstream of the inner field cage.

Warning: An even higher misalignment of the high voltage between inner and outer field cages, from 1.6% up to perhaps 2.3%, cannot be excluded at this point in time. Inter-calibration of the respective high voltage units is in progress [5].

Table 3: Transverse electric field strengths (in V/m). A positive sign means pointing to the outer field cage, a negative sign means pointing toward the TPC axis.

	at inner radius	at outer radius
Cosmics	-0.27	0.12
Interaction secondaries	-26.	3.4
Beam muons	-3.7	0.94
Downstream beam particles	3.1	0.40
High voltage misalignment	176.	176.

Conclusion 5: The by far largest transverse electric field component is caused by the high voltage misalignment.

7 Transverse electron drift velocities

Table 4 gives the transverse electron drift velocities according to Equations 4 for the electric field inhomogeneities, and Equations 6 for the magnetic field inhomogeneity.

Table 4: Transverse electron velocities in m/s. The x coordinate is equivalent to the r coordinate, the y coordinate is equivalent to the $r{\cdot}\phi$ coordinate. In case of a double sign, the upper sign refers to positive beam polarity, and the lower sign to negative beam polarity.

	small radius		large radius	
	v_{x}	v_{y}	v_{x}	v_{y}
Cosmics	0.10	$\pm$0.34	-0.05	$\mp$0.15
Interaction secondaries	10.	$\pm$33.	-1.3	$\mp$4.3
Beam muons	1.4	$\pm$4.7	-0.36	$\mp$1.2
Downstream beam particles	-1.2	$\mp$3.9	-0.15	$\mp$0.51
High voltage misalignment	-68.	$\mp$223.	-68.	$\mp$223.
Magnet inhomogeneity	92.	$\mp$28.	458.	$\mp$139.

8 Distortions of the r and $r{\cdot}\phi$ coordinates

Using Equations 5, we calculate the 'electric' distortions in the x and y coordinates which result from the transverse components of the electric field.

Without loss of generality, we consider the effect on charges which drift in the horizontal half-plane ($y = 0$, $x > 0$) toward the pad plane. We illustrate the distortions at two x positions: at the inner radius and at the outer radius of the active TPC volume. Because of the azimuthal symmetry of the HARP TPC, the distortion along the x coordinate represents a distortion along the r coordinate, and the distortion along the y coordinate represents a distortion along the $r{\cdot}\phi$ coordinate.

Except in case of the high voltage misalignment, a typical drift length of 1 m has been chosen to calculate 'electric' distortions in the r and $r{\cdot}\phi$ coordinates. For the high voltage misalignment, the length of the inner field cage has been taken as drift length.

Next, using Equations 7, we calculate the 'magnetic' distortions in the r and $r{\cdot}\phi$ coordinates which result from the transverse components of the magnetic field.

Figure 1 shows the inhomogeneity of the magnetic solenoid field as used in track reconstruction and Monte Carlo simulation [6]. To estimate the size of expected effects, we take as average transverse component at small radius 0.2% of the longitudinal magnetic field, and at large radius 1%, and take both vectors pointing toward the TPC axis.

Inspection of Figure 1 shows that the net distortion for a given cluster will strongly depend on its position inside the actve TPC volume, especially at large radii, and so will the sign of the effect. The distortion given below should be considered a typical value, actual distortions

can be larger or smaller, and can have opposite sign in the $r \cdot \phi$ coordinate.

A typical drift length of 1 m has been taken for the calculatiom of the 'magnetic' distortions in the r and $r \cdot \phi$ coordinates.

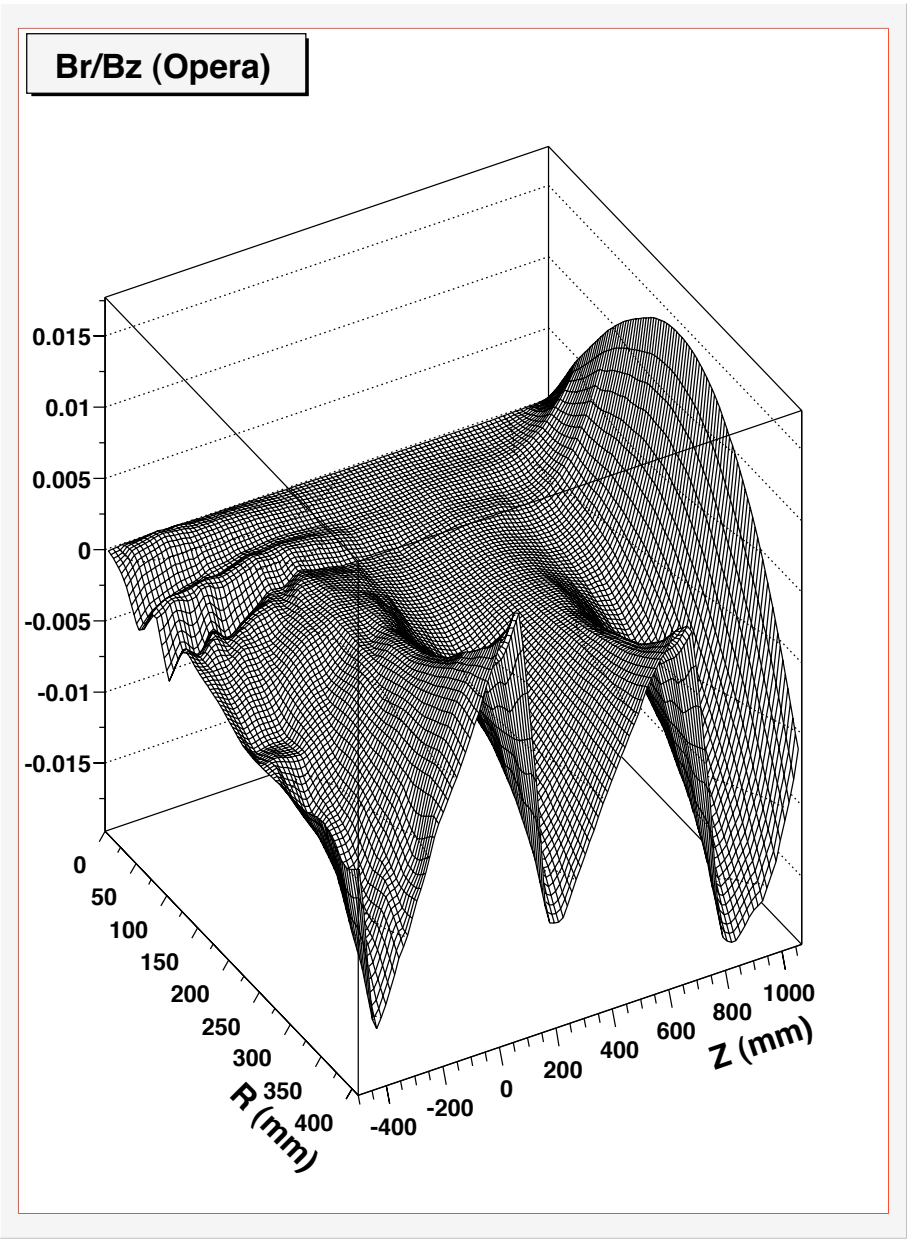

Figure 1: Inhomogeneity of the solenoidal magnetic field.

Table 5 gives the results of the distortions in mm. We recall that in case of a double sign in the distortion, the upper sign refers to the magnetic field orientation $\vec{B} = (0, 0, B_z)$ with $B_z > 0$, which is the field polarity for positive beam. The lower signs refers to the opposite magnetic field orientation which is the field polarity for negative beam.

All numbers should be compared to $\simeq 0.5$ mm which is the TPC's $r \cdot \phi$ precision under next-to-ideal circumstances. It is clear that some distortions are much greater and, therefore,

must be corrected with adequate accuracy.

Table 5: Transverse distortions in mm. The x coordinate is equivalent to the r coordinate, the y coordinate is equivalent to the $r{\cdot}\phi$ coordinate. In case of a double sign, the upper sign refers to positive beam polarity, and the lower sign to negative beam polarity.

	small radius		large radius	
	Δx	Δy	Δx	Δy
Cosmics	0.	$\pm$0.01	0.	0.
Interaction secondaries	0.20	$\pm$0.66	-0.03	$\mp$0.09
Beam muons	0.03	$\pm$0.09	-0.01	$\mp$0.02
Downstream beam particles	-0.02	$\mp$0.08	0.	$\mp$0.01
High voltage misalignment	-0.54	$\mp$1.79	-0.54	$\mp$1.79
Magnet inhomogeneity	1.83	$\mp$0.56	9.15	$\mp$2.79

Figure 2 shows the resulting distortions, illustrated as vectors on the same relative scale, of the x and y coordinates of clusters at the inner and outer radius of the active TPC volume.

Conclusion 6: While all (uncritical) distortions in the r coordinate do not change sign when the magnetic field is reversed (i.e., in our data taking mode, with beam polarity), the (critical) distortions in the $r{\cdot}\phi$ coordinate do change sign.

Conclusion 7: The largest distortions arise from the inhomogeneity of the magnetic field. Fortunately, this effect is stable and can be well corrected. Another fortunate fact is that the largest effect is on the (uncritical) r coordinate.

Except stating that expected effects are large, especially at large radius, no general predictions for the magnitude and sign of the effect for a specific track can be made without taking the precise magnetic field map into account.

Conclusion 8: The second-largest distortion arises from the misalignment of the high voltage between the inner and outer field cages. Fortunately, also this effect is stable and can be well corrected. Unfortunately, the largest effect is on the (critical) $r{\cdot}\phi$ coordinate.

Regarding the $r{\cdot}\phi$ distortion, this latter effect produces for positive beam polarity and when looking downstream, an anti-clockwise movement of clusters. For negative beam polarity, the effect changes sign because of the reversed magnetic field.

In positive beam polarity, positively charged secondaries bend anti-clockwise. The distortion will cause the interaction vertex to appear outside the fitted circle for positive secondaries, and inside for negative secondaries. In negative beam polarity, positively charged secondaries bend clockwise, however the distortions have opposite sign, too. Hence, the above feature is true irrespective of beam polarity.

Nachtigall, ick hör dir trapsen!

Conclusion 9: Since the distortions from magnetic field inhomogeneity and the

high voltage misalignment are present during all the data taking, with no time variation, they can be calculated and corrected with the help of a 'correction map' which gives the r and $r \cdot \phi$ distortions for a grid of points inside the active TPC volume. The 'correction map' is obtained through numerical integration of Equations 4 and 6. The correctness of the calculation (the Langevin formalism is believed to be a good approximation for the operating conditions of the HARP TPC, but should not be expected to be perfect) can be confirmed by laser data taken routinely during data taking. The determination of the 'correction map' and the analysis of the laser data are the next steps which will be undertaken.

Conclusion 10: Likely, the third-largest distortion arises from ion build-up from charged secondaries. The quantitative size of this effect is determined by the transparencies of the gating grid in open and closed mode which is yet unknown. The upper limits suggest that the effect cannot be neglected. Unfortunately, the effect depends on beam intensity, beam momentum, and target.

Conclusion 11: While the distortions from cosmics is definitively negligible, the effects from beam muons and from downstream beam particles are likely so.

Conclusion 12: While the main distortions are expected to be stable during the spill, this is not expected for the effect from ion build-up from interaction secondaries. Here, two effects will conspire: (i) the ion cloud near the target region will slowly extend toward the high voltage membrane; (ii) the finite transparency of the gate will produce another ion cloud which will slowly extend from the gate wires toward the high voltage membrane. During spill duration, both ion clouds produce a steady increase of distortion, which should show up especially for clusters at large z.

The effect can be simulated with sufficient precision and corrected with the help of yet another 'correction map', which, however, is not a once-for-ever set of numbers but depends on the data taking parameters. Again, the correction can be confirmed by laser data.

9 Summary

Non-neglibible coordinate distortions in the TPC must be anticipated. Their correction is unavoidable and constitutes an urgent task.

However, with the investment of enough sweat and tears, corrections can be calculated such that the final precision of TPC coordinate measurement will not be significantly degraded. Calculated corrections can be confirmed by existing laser data.

References

[1] We thank R. Veenhof for pointing out the correct origin of the 'drift' $E \times B$ effect.

[2] 'Particle Detection with Drift Chambers', W. Blum and L. Rolandi (Springer, 1993).

[3] We thank M. Chizhov who ascertained this correspondence with data.

[4] Particle Data Group, Phys. Rev. **D66** (2002) 1; see p. 211; we wish to thank M. Chizhov who pointed to inconsistencies in sign conventions which in turn lead to the revised version of this Memo.

[5] We thank L. Linssen for having brought the high voltage misalignment problem to our attention, and for ongoing calibration work to ascertain the precise size of misalignment.

[6] We thank E. Boter and L. Linssen who produced the field map with the OPERA program and verified it against the measured field map. We also thank Y. Nefedov who made the field map available in analysis programs.

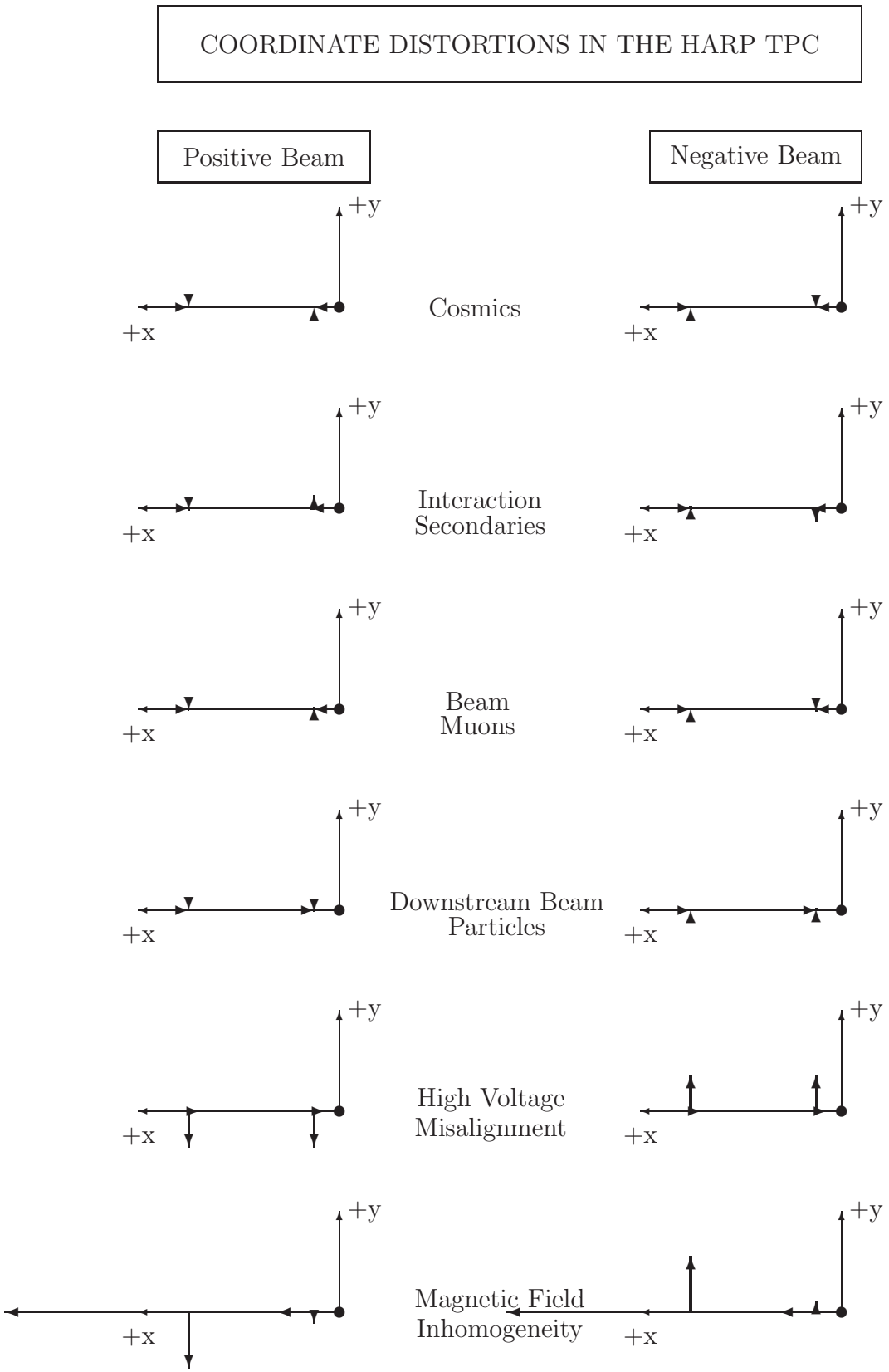

Figure 2: Vectors illustrating the coordinate distortions in the TPC, for small and large radius. Relative magnitude and sign correspond to the results given in Table 5.